ev. Mexicana Astron. Astrof., 21, 89-98 (1990)

VIOLENT RELAXATION, DYNAMICAL INSTABILITIES AND THE FORMATION OF ELLIPTICAL GALAXIES

(Invited Talk)

Luis A. Aguilar

Instituto de Astronomía
Universidad Nacional Autónoma de México

RESUMEN: El problema de la formación de galaxias elípticas por medio de colapso gravitacional sin disipación de energía es estudiado usando un gran número de simulaciones numéricas. Se muestra que este tipo de colapsos, partiendo de condiciones iniciales frías donde la energía cinética inicial representa sólo un 5%, o menos, de la energía potencial inicial, produce sistemas relajados de forma triaxial muy similares a las galaxias elípticas reales en sus formas y perfiles de densidad en proyección. La forma triaxial resulta de la acción de una inestabilidad dinámica que aparece en sistemas dinámicos dominados por movimientos radiales, mientras que el perfil de densidad final es debido al llamado relajamiento violento que tiende a producir una distribución en espacio fase única. Estos dos fenómenos tienden a borrar los detalles particulares sobre las condiciones iniciales y dan lugar a una evolución convergente hacia sistemas realistas, esto hace innecesario el uso de condiciones iniciales especiales (excepto por la condición de que estas deben ser frías). Las condiciones iniciales frías producen los movimientos radiales y fluctuaciones de la energía potencial requeridos por ambos fenómenos.

ABSTRACT: The problem of formation of elliptical galaxies via dissipationless collapse is studied using a large set of numerical simulations. It is shown that dissipationless collapses from cold initial conditions, where the total initial kinetic energy is less than 5% of the initial potential energy, lead to relaxed triaxial systems very similar to real elliptical galaxies in projected shape and density profiles. The triaxial shape is due to the presence of a dynamical instability that appears on systems dominated by radial orbits, while the final density profile is due to violent relaxation that tends to produce a unique distribution in phase space. These two phenomena erase memory of the initial conditions and produce a convergent evolution toward realistic systems, thus making unnecessary the use of special initial conditions (other than the condition of being cold). Cold initial conditions generate the radial orbits and large potential energy fluctuations necessary for both phenomena and are thus sufficient.

Key words: **GALAXIES-DYNAMICS – GALAXIES-ELLIPTICAL – GALAXIES-FORMATION**

. INTRODUCTION

Elliptical galaxies are deceivingly simple, their surface brightness profiles are reasonably well described y a unique fitting formula first proposed by de Vaucouleurs (de Vaucouleurs 1948, 1953):

$$\Sigma(r) = \Sigma_e \exp\{-7.67[(r/r_e)^{1/4} - 1]\}, \quad (1)$$

hose only degrees of freedom are the normalizations in length (given by r_e, the radius enclosing half of the light) and otal light (given by Σ_e, the surface brightness profile at the half-light radius). Their shapes, as seen in projection, are emarkably featureless, with elliptical isophotes that range from circular to a maximum axis ratio of ~ 0.5. When we ealize that the two–body relaxation timescale for these systems is very large compared with the age of the universe, e are confronted with the problem of explaining the origin of these very regular observed properties. We can invoke

very special initial conditions, like secondary infall (Gott, 1975) and highly flattened configurations (Binney, 1976; Aarseth and Binney, 1978), to explain these regularities; or we can attribute them to a phenomenon that acts during the formation, or subsequent evolution of galaxies, and funnels the evolution of these systems toward the observed distribution of shapes and density profiles, like mergers of disk galaxies in the high density environments of rich clusters of galaxies (Toomre and Toomre, 1972). The second possibility is more attractive because no "fine" tunning of the initial conditions is required, but we now need a physical mechanism that provides the desired convergent evolution.

A possible formation scenario for elliptical galaxies is dissipationless collapse whereby a protogalaxy, out of virial equilibrium, collapses without dissipating energy. Although such coherent non–dissipational collapse is a somewhat idealistic situation, it is nevertheless important to study it because its simplicity can allow us to understand it throughly; the insight gained from its study can then guide us when we move to more realistic situations. Furthermore, the effect of a physical mechanism of the type we are interested, namely one that erases memory of the initial conditions, should be largely unaffected by some or most of the simplifications assumed.

Among the first numerical simulations of dissipationless collapse we have those of Hénon (1964), Peebles (1970), Bouvier and Janin (1970) and Gott (1973). These early experiments confronted immediately a serious impasse: the resulting relaxed systems exhibited a surface density profile too steep ($\Sigma \propto r^{-3}$) to agree with those of elliptical galaxies. This motivated the work of Gott (1975) who presented a model where *secondary infall* from the loosely bound material that surrounds the protogalaxy produces a flatter, more extended density profile. A few years later, van Albada (1982) in a groundbreaking contribution, presented a series of dissipationless collapse experiments using a new generation of N–body codes with a much larger spatial dynamical range than those in previous works. His initial conditions where similar to those of preceding simulations, but the collapse factors were significatively larger; interestingly, he obtained relaxed systems whose density profiles were closer to a de Vaucouleurs law as the collapse factor increased. It thus seemed that the difficulty that had plagued early simulations was not inherent to the collapse, but to the rather mild collapses being simulated due to lack of resolution. Van Albada's result has been confirmed by, among others, McGlynn (1984) and Villumsen (1984) who have also demonstrated that this result is not affected by the use of rotating or non–spherical initial conditions. It seems that a large enough collapse factor, which results in a more efficient violent relaxation, leads to a de Vaucouleur's profile.

A few years later, Merritt and Aguilar (1985) showed that collapses from cold, spherical initial conditions, those with the largest collapse factors, are affected by a non–radial instability that acts on systems with a large fraction of radial orbits. This *radial orbit instability*, whose effect is to produce triaxial systems, was first studied by Antonov (1973) for the extreme case of a system made entirely of radial orbits, and then extended to more general systems by Polyachenko and Shukhman (1981) and Fridman and Polyachenko (1984). Since the large collapse factors that are necessary to produce realistic density profiles seem to also favour the appeareance of this instability, it seems that the simplest formation scenario, namely cold dissipationless collapse, can at the same time produce systems with the right shape and density profiles.

II. THE RADIAL ORBIT INSTABILITY

Figure 1 shows the collapse of an initially spherical, $\rho \propto r^{-1}$, non–rotating protogalaxy, with random gaussian velocities such that the initial virial ratio is $\log(2T/W) = -1.0$. We note that in less that two crossing times (measured at the half–mass radius), the system departs form its initial spherical symmetry and becomes elongated. This simulation is to be contrasted with that of Figure 2, started from the *same* initial conditions but with the magnitude of the initial velocity vectors scaled down to give an initial virial ratio of $\log(2T/W) = -0.75$. It is clear that the outcome of these, otherwise quite similar initial conditions, is very different. These simulations have been performed with an N–body code that computes forces using an expansion of the potential in spherical harmonics up to $l = 3$ order (Aguilar and Merritt, 1990). The same result is obtained when performing the experiments with a completely different numerical technique, namely an Aarseth–type, direct integration code (Aguilar, Merritt and Duncan, 1986).

Aguilar and Merritt (1990) have studied in detail the role of this instability for dissipationless collapses started from a variety of initial conditions. Their initial conditions have various amounts of random and rotational kinetic energies, as well as shapes. They conclude that the only parameter that seems to be relevant for the appeareance of the instability is the total initial virial ratio, regardless of the relative contributions of rotational and random motions to the kinetic energy: All initial conditions whose initial virial ratios are 0.1, or less, are affected. This effect can clearely be seen in Figure 3, where the distribution of final shapes for a grid of non–rotating, oblate, initial conditions is shown. The grid of initial conditions is squematically shown in the upper right corner of the figure, with the initial virial ratio along the abscissa, and the axis ratio of the initial oblate shape along the ordinate. The final shape is characterized by the triaxiality index $\tau \equiv (b-c)/(a-b)$, where $a > b > c$ are the eigenvalues of the inertia tensor computed for the 80% most bound particles only. The triaxiality index varies from 0, for a perfectly prolate shape, to 1, for a perfectly oblate one; being equal to 0.5 for a triaxial object whose intermediate axis is equal to the mean of the other two. Since τ is not defined for a spherical object, it is necessary to introduce a second parameter, for this we have adopted the short to

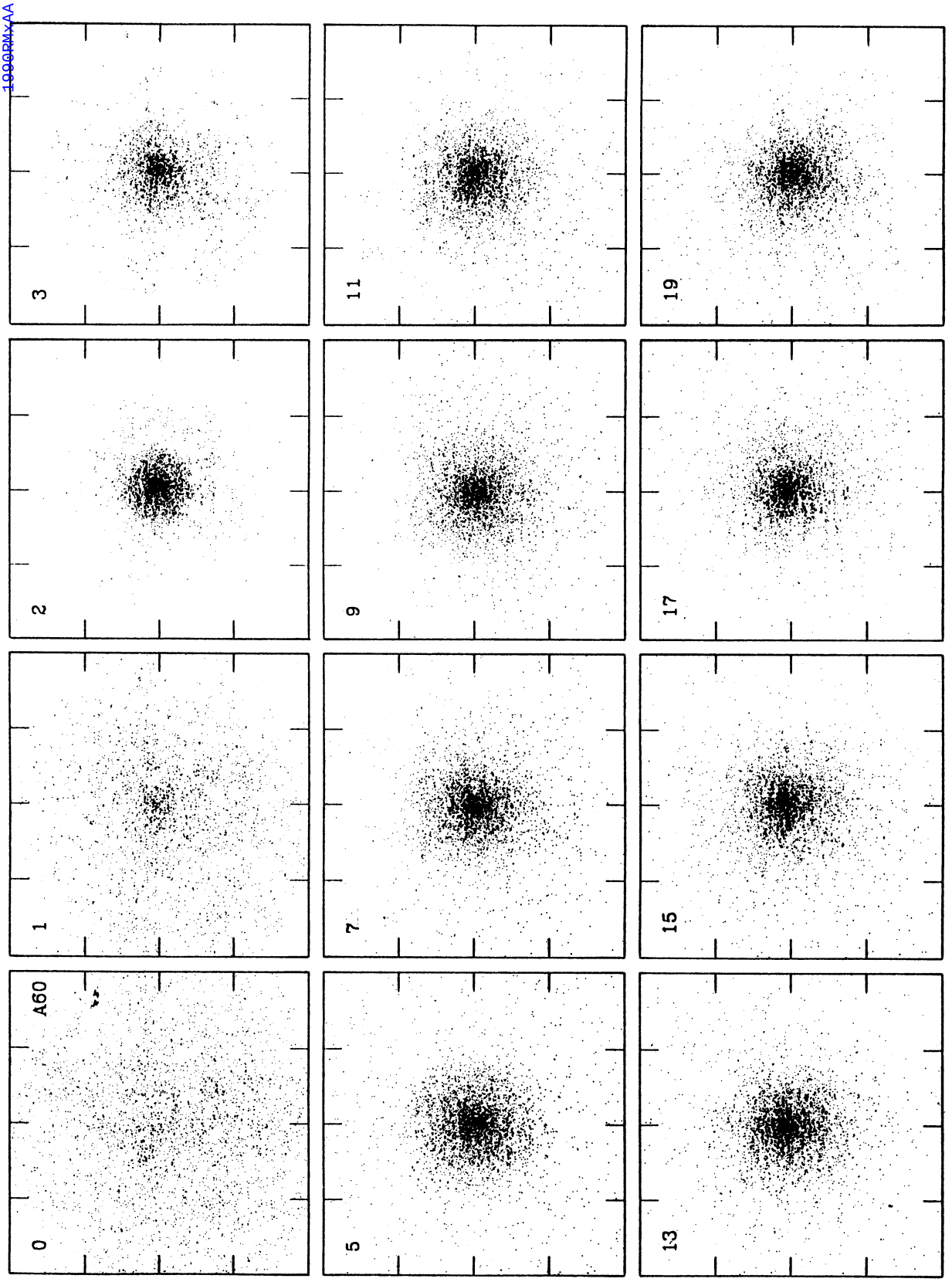

Fig. 1. Numerical simulation of the dissipationless collapse and subsequent relaxation of a initially spherical, non-rotating protogalaxy of 5000 particles and a $\rho \alpha r^{-1}$ density profile. The initial velocity vectors are randomly drawn from an isotropic gaussian distribution whose dispertion is such that initial virial ratio is log(2T/W) = −1.0. The frames are equally spaced at half free-fall times (measured at the half-mass radius) in the upper row, and twice as long in the lower two rows. The view is from a position such that the maximum elongation is apparent.

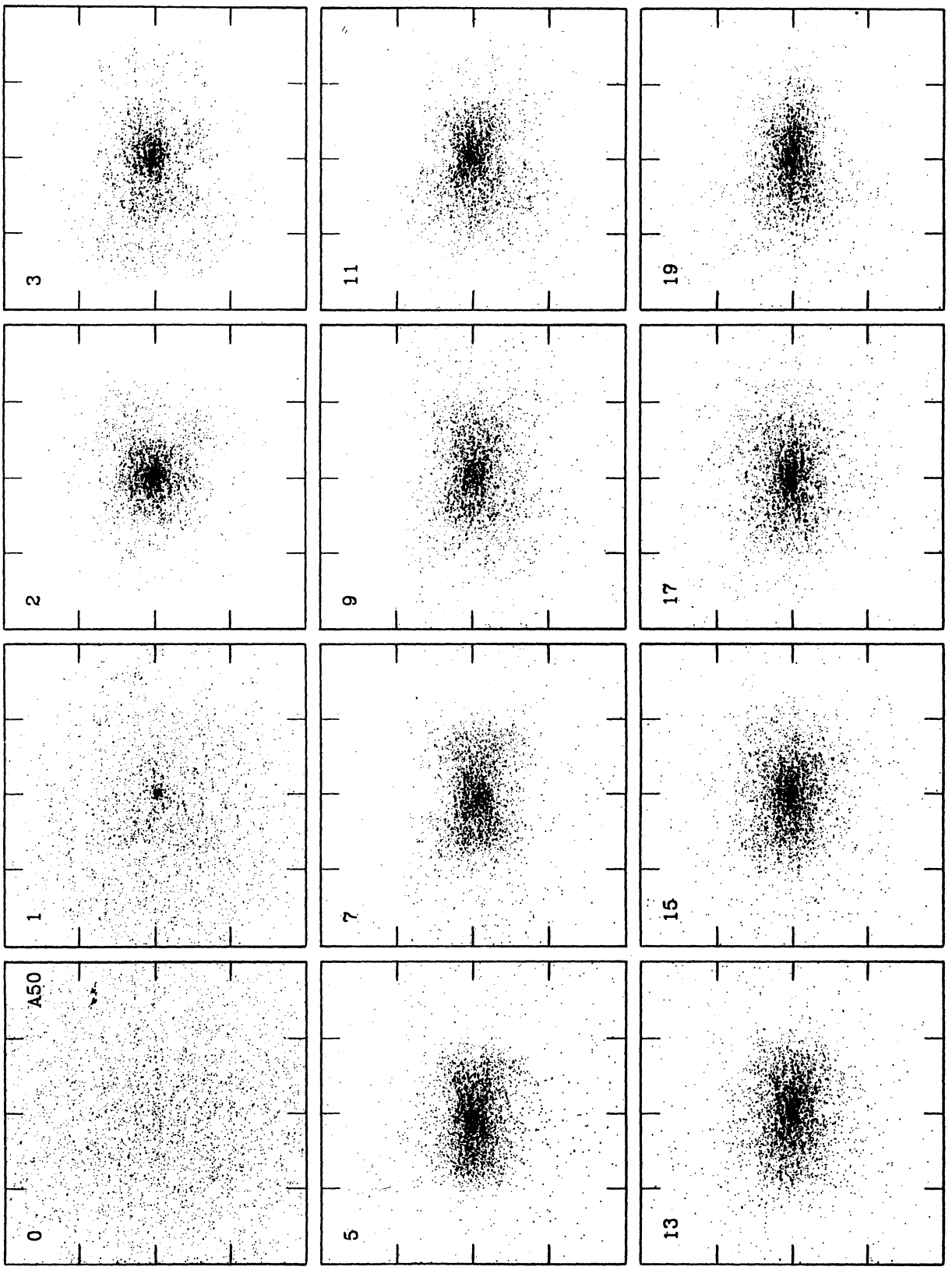

Fig. 2. Similar to Figure 1, but the initial velocity vectors been scaled down so that the virial ratio of the initial configuration is $\log(2T/W) = -0.75$.

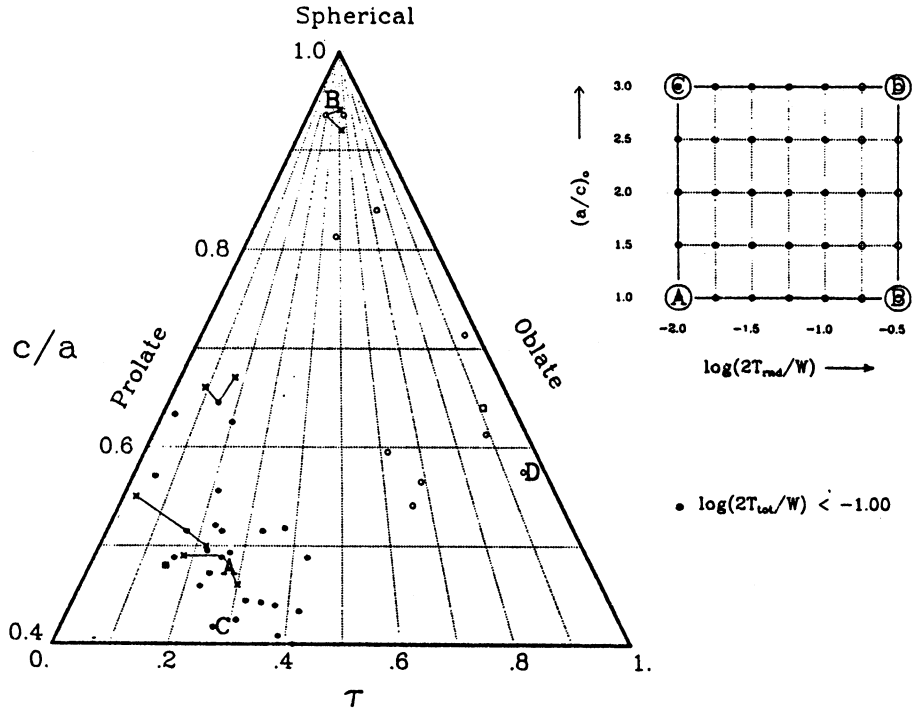

Fig.3. Final shape of the relaxed systems that result from the dissipationless collapse from non–rotating, oblate initial conditions. The initial grid of models, whose parameters are the initial virial ratio and long to short axis ratio, is squematically shown in the upper right corner of the figure. The shapes are shown in a triangular diagram where the abscissa is the triaxiality index τ, and the ordinate is the final minor to major axis ratio (c/a) (see text). Filled circles are collapses from "cold" initial conditions whose initial virial ratios are less or equal than 0.1, filled circles are collapses from warmer initial conditions. A few experiments have been repeated with different random realizations of the same initial model, they are shown as stars connected to their respective parent model.

long axis ratio c/a, that varies from 0, for a flat shape, to 1, for a spherical one. The shape of the final relaxed system is then represented as a point in the triangular diagram of Figure 3, where a sphere would be at the upper vertex, flat ellipsoids at the base (not shown), prolate objects along the left edge, and oblate ones along the right edge of the triangle.

Filled circles are collapses started from "cold" initial conditions (i.e., $(2T/W) \leq 0.1$), open circles are collapses from warmer intial conditions. We can see that filled and open circles occupy different regions of the diagram, with open circles running along the oblate edge of the triangle while filled circles have "forgotten" their initially oblate shape and present a distribution of shapes between triaxial and prolate. The same effect is seen for a grid of initially spherical, rotating initial conditions, shown in Figure 4. The grid of initial conditions, whose parameters are the rotational and random kinetic energies, is shown in the upper right part of the figure. The difference between open and filled circles is the same as in the previous figure, with both, random and rotational kinetic energies taken together.

III. SURFACE DENSITY PROFILES

Another feature of cold collapses, first noted by van Albada (1982), is that as the collapse factor increases, the final projected density profiles are better described by a de Vaucouleurs law. This can be seen in Figure 5, where the surface density profile is shown for the relaxed systems that result from the collapses of spherical, non–rotating initial conditions with various amounts of initial random motions. The large fluctuations for $(r/r_e) > 10$ are not significant, since the local dynamical timescale for these outlying regions exceeds the time span of the simulation. The approach to a de Vaucouleurs profile is smooth, with no clear jump, as in the case of the radial orbit instability.

Although the collapses that suffer the radial orbit instability are the same whose surface density profiles are best described by the de Vaucouleurs profile, this two phenomena are independent. This can be seen in Figure 6, which shows, to the left, the residuals of the fits of Figure 5, and to the right, the analogous residuals for collapses from

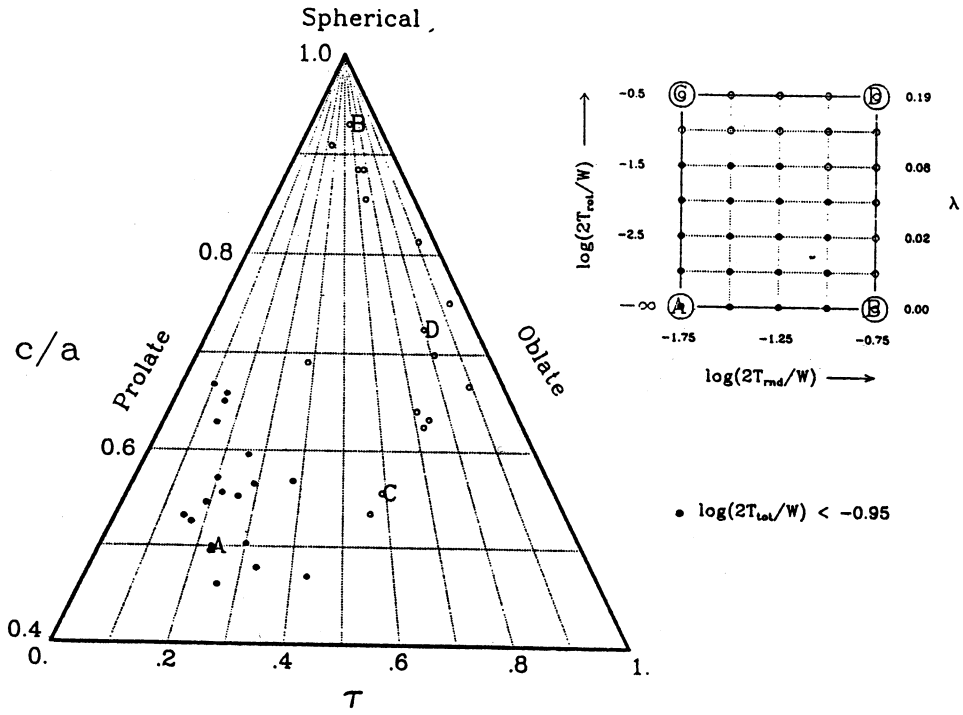

Fig. 4. Same as Figure 3, but for a grid of rotating, spherical initial conditions.

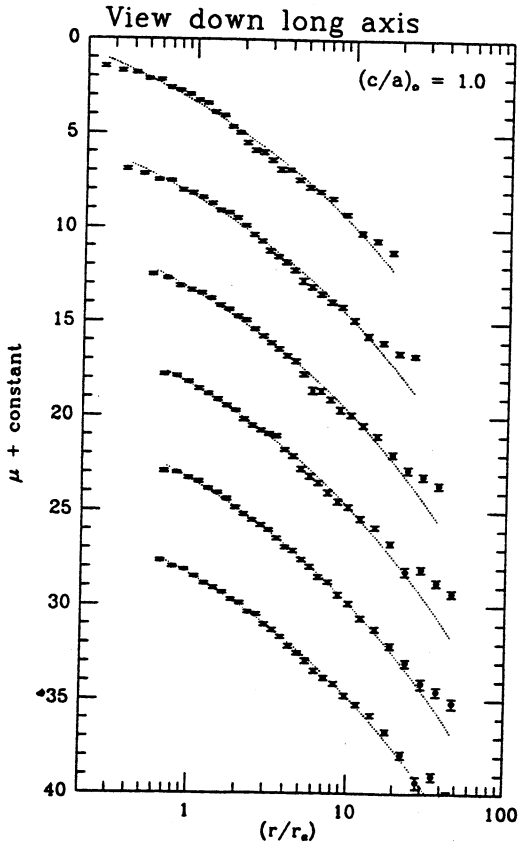

Fig. 5. Surface density profiles in magnitudes for the relaxed systems that result from the collapse of spherical, non-rotating initial conditions with logarithm of the initial virial ratio from −0.75 (top), to −1.75 (bottom), at intervals of 0.25. Each point is shown with its Poissonian error bar. The dotted lines are the de Vaucouleurs profiles fitted to each profile; only points within $10r_e$ have been used for the fit. The profiles have been shifted vertically for clarity.

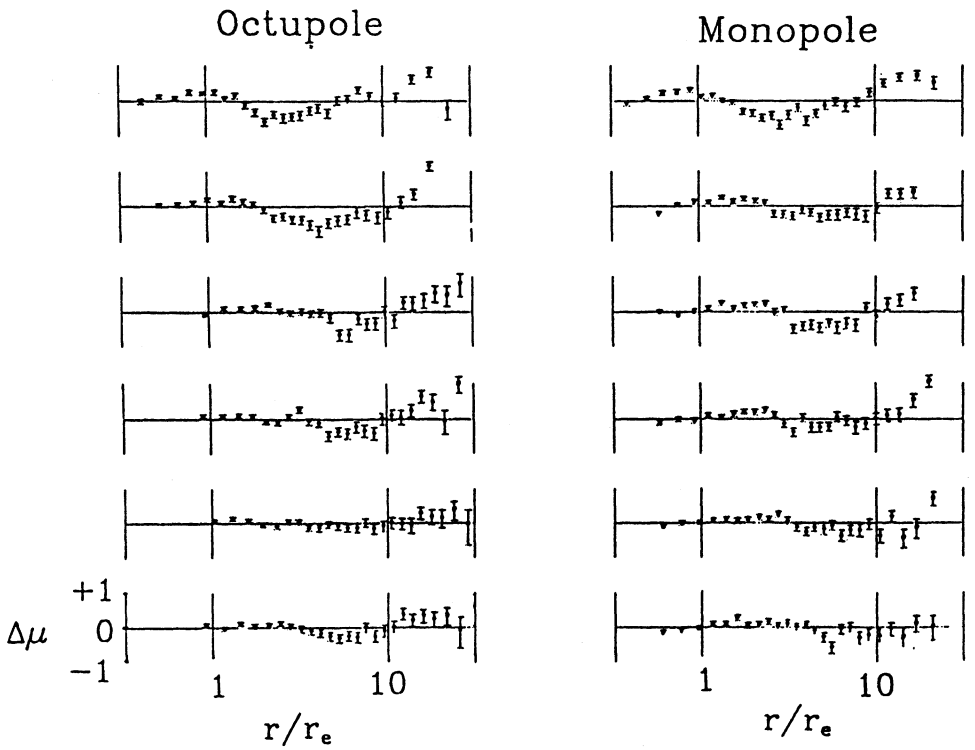

g. 6. Residuals in magnitudes of the fits shown in Figure 5 (left), and the analogous quantities for collapses started from the same initial conditions it with a monopolar N–body code that enforces spherical symmetry (right). The models appear in the same order as that in Figure 5.

ıe same initial conditions, but evolved with an N–body code that enforces spherical symmetry. In the latter case, the ıdial orbit instability is inhibited, nevertheless, the same trend is apparent: colder initial conditions lead to better de aucouleurs profiles. Merritt and Aguilar (1985) have shown that the reverse can also be true, they found that for quilibrium systems dominated by radial motions, the radial orbit instability changes the spatial shape of the model ithout changing the density profile.

These results suggest that it is the large relaxation that the system undergoes when collapsing from cold ıitial conditions what is responsible for the de Vaucouleurs profile, while the radial orbit instability is produced by the xcess of radial motions produced by a large collapse factor, thus, although in the case of dissipationless collapses the vo phenomena have a common origin, their causes are different.

V. PHASE SPACE DISTRIBUTION

Systems formed from collapses that are forced to remain spherical are ideal to study the phase space istribution that arises from violent relaxation. A spherical system has a phase space structure that is easier to nderstand than that of a fully three–dimensional model because its integrals of motion are much simpler. Since ıe trend toward the de Vaucouleurs density profile obtained in cold collapses is unaffected by the geometry forced pon the simulation, the analysis of the phase space structure of these models may shed some light on the origin of this rofile.

Tremaine (1987) has suggested that the phase space distribution first suggested by Bertin and Stiavelli 1984, 1987):

$$f(E, J^2) = f_o |E|^{3/2} \exp\{-\beta E - \alpha J^2\}, \tag{2}$$

a natural outcome for a system that undergoes violent relaxation. The natural tendency of the relaxation process toward the Maxwellian form given by the exponential dependence in energy, but, due to the large spectrum of ynamical timescales, the relaxation process is never complete and different regions of phase space are populated in

inverse proportion to their dynamical timescale ($T_{dyn} \propto |E|^{-3/2}$). Since the relaxation process takes place mostly in t central regions, orbits with large angular momentum are unlikely to be populated by the relaxation process, thi modelled with the exponential cut-off in J^2 in equation (2).

Merritt, Tremaine and Johnstone (1989) have built models corresponding to this phase sp distribution but with "negative temperature" (i.e., $\beta < 0$). These models have the property that their velocity anisotrc increases as the concentration increases, which is exactly the trend expected to arise in a dissipationless collapse. T trend is shown in Figure 7 which shows the relation between velocity anisotropy and concentration for these mod Also shown in this figure, are the concentration and anisotropy of systems that result from spherical collapses of no rotating initial conditions whose initial virial ratio range from 0.01 to 0.30. As we move from warmer to colder collaps the points move close and parallel to the relation defined by the theoretical models, toward higher anisotropy a concentration. The projected density profiles of these theoretical models resemble quite closely a de Vaucoule profile within the observable range.

Cold initial conditions are also necessary to produce a de Vaucouleurs profile for a system that collap without dissipation, because, in this case, the fine-grained phase space density remains constant through the collap Since a de Vaucouleurs model is very concentrated, this means that the initial conditions should also have a large ph space density to start with. This result has been pointed out by May and van Albada (1984) and has been investigat in more detail by Tremaine, Hénon and Lynden-Bell (1986) who concluded that to explain systems as concentrated real galaxies, a very cold initial state ($(2T/W) \leq 0.02$) is required. This effect can be seen in Figure 5, where the dens profiles of systems formed from warmer collapses are systematically below the de Vaucouleurs profile in the innerm regions.

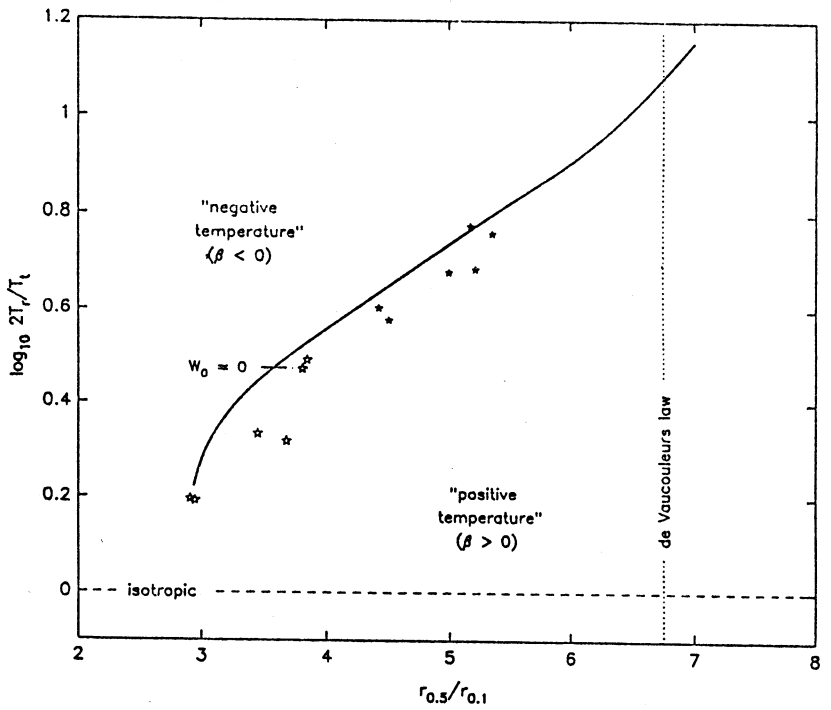

Fig. 7. The relation between velocity anisotropy, measured as the ratio of twice the kinetic energy in radial motions to the kinetic energy i tangential motions, to the model concentration, measured as the ratio of the half-mass radius to the one that encloses 10% of the mass. Th solid lined is the location of models constructed from equation (2), with the horizontal tick mark indicating the boundary between positive an negative temperature models. The stars are the systems obtained from spherical collapses of non-rotating initial conditions with various amou of random motions. Filled stars indicate systems whose initial virial ratio is less than 0.1. The concentration of a de Vaucouleurs profile is indicate as a reference.

V. DARK HALOS

According to some scenarios for the formation of the large scale structure of the universe (e.g., the col dark matter hypothesis), the baryonic luminous material that makes the observable part of galaxies collapses within th potential wells produced by the density fluctuations of dark, weakly interacting particles.

We have seen that the dissipationless collapse of cold initial conditions leads to triaxial configurations; lthough the extent to which this model is affected by the role of dissipation in the formation of the luminous component f elliptical galaxies is an open question, the dissipationless model is a good model for the collapse and virialization of dark halo made of weakly interacting particles. The present results thus seem to indicate that dark halos are triaxial. inney (1987) has discussed the consequences of such triaxial halos on the observable luminous component. Among ıese consequences, we have that a triaxial halo can sustain, or even produce, the warps often seen on some disk galaxies; ıis effect can come about through a misalignment between the principal axes of the dark and luminous components Dekel and Shlosman 1983, Toomre 1983). A triaxial potential admits stable closed orbits on planes orthogonal to its ıinor and major axes, this can provide an explanation to the phenomenon of "polar rings" observed in some galaxies Fohline, Simonson and Caldwell 1982, van Albada, Kotanyi and Schwarzchild 1982). Finally, a triaxial potential admits larger proportion of highly elongated orbits than an axisymmetric one, this could facilitate the trapping of satellite alaxies by luminous galaxies (Binney 1987), or promote the destruction of globular clusters in disk galaxies through dal shocks produced by the central bulge of the galaxy (Aguilar, Hut and Ostriker 1982).

If, by some unknown mechanism, dark halos remain spherical, the question arises as to whether the alo could inhibit the formation of a triaxial luminous component that forms via dissipationless collapse. This has been ıvestigated by Muzzio, Lecar and Aguilar (1990), who have run collapse experiments within an underlying, fixed, ɔherical potential, for luminous to dark mass ratios of up to one to 99. They find that in all cases, triaxial systems re inevitable, but their formation is delayed as the mass of the galaxy becomes negligible. Thus even in the extreme ıse of a spherical halo, a luminous component formed via dissipationless collapse will be affected by the radial orbit ıstability and end up as a triaxial object.

I. CONCLUSIONS

Dissipationless collapses from cold initial conditions ($(2T/W) \leq 0.1$) lead to relaxed, triaxial systems whose rojected density profiles resemble those of real elliptical galaxies. The triaxial shape is attained through the action f the radial orbit instability, which is promoted by the dominance of radial orbits produced during the collapse. The ırface density profile is produced by the effect of violent relaxation, which seems to lead to a phase space distribution ith an exponential dependence in energy. These results are unaffected by the initial shape or amount of rotation of ıe initial conditions, provided that the upper limit on the initial virial ratio is not exceeded. This model may provide s with a plausible mechanism for the formation of elliptical galaxies, but the effect of inhomogeneities and dissipation ave to be studied. These results also suggest that a dark halo made of collisionless particles that forms via gravitational ɔllapse is very likely to be triaxial.

EFERENCES

arseth, S.J. and Binney, J. 1978, *M.N.R.A.S.*, **185**, 227.

guilar, L., Hut, P., and Ostriker, J.P. 1988, *Ap.J.*, **335**, 720.

guilar, L., Merritt, D., and Duncan, M. 1987, in *IAU Symposium No. 127, Structure and Dynamics of Elliptical Galaxies*, ed. T. de Zeeuw (Dordrecht: D. Reidel).

guilar, L. and Merritt, D. 1990 *Ap.J.*, **354**, in press.

ntonov, V.A. 1973, in *The Dynamics of Galaxies and Star Clusters*, ed. G.B. Omarov (Nauka, Alma Ata), p. 139.

ertin, G. and Stiavelli, M. 1984, *Astr. and Ap.*, **137**, 26.

ertin, G. and Stiavelli, M. 1987, in *IAU Symposium No. 127, Structure and Dynamics of Elliptical Galaxies*, ed. T. de Zeeuw (Dordrecht: D. Reidel).

inney, J. 1976, *M.N.R.A.S.*, **177**, 19.

inney, J. 1987, in *IAU Symposium No. 117, Dark Matter in the Universe*, eds. J. Kormendy and G.R. Knapp, (Dordrecht: D. Reidel).

ɔuvier, P. and Janin, G. 1970, *Astr. and Ap.*, **5**, 127.

ekel, A. and Sloshman, I. 1983, in *IAU Symposium No. 100, Internal Kinematics and Dynamics of Galaxies*, ed. L. Athanassoula, (Dordrecht: D. Reidel).

: Vaucouleurs, G. 1948, *Ann. d'Astrophys.*, **11**, 247.

de Vaucouleurs, G. 1953, *M.N.R.A.S.*, **113**, 134.

Fridman, A.M. and Polyachenko, V.L. 1984, *Physics of Gravitating Systems*, Vols. 1 and 2 (New York: Springer Verlag).

Gott, J.R. III 1973, *Ap.J.*, **186**, 481.

Gott, J.R. III 1975, *Ap.J.*, **201**, 296.

Hénon, M. 1964, *Ann. d'Astrophys.*, **27**, 83.

May, A. and van Albada, T.S. 1984, *M.N.R.A.S.*, **209**, 15.

McGlynn, T. 1984, *Ap.J.*, **281**, 13.

Merritt, D. and Aguilar, L. 1985, *M.N.R.A.S.*, **217**, 787.

Merritt, D., Tremaine, S., and Johnstone, D. 1989, *M.N.R.A.S.*, **236**, 829.

Muzzio, J.C., Lecar, M., and Aguilar, L. 1990, in preparation. Peebles, P.J.E. 1970, *A.J.*, **75**, 13.

Polyachenko, V.L. and Shukhman, I.G. 1981, *Astr. Zh.*, **58**, 933 (translated in *Soviet Astr.*, **25**, 533).

Tohline, J.E., Simonson, G.F., and Caldwell, N. 1982, *Ap.J.*, **252**, 92.

Toomre, A. and Toomre, J. 1972, *Ap.J.*, **178**, 623.

Toomre, A. 1983, in *IAU Symposium No. 100, Internal Kinematics and Dynamics of Galaxies*, ed. L. Athanassoula, (Dordrecht D. Reidel).

Tremaine, S., Hénon, M., and Lynden–Bell, D. 1986, *M.N.R.A.S.*, **219**, 285.

Tremaine, S. 1987, in *IAU Symposium No. 127, Structure and Dynamics of Elliptical Galaxies*, ed. T. de Zeeuw, (Dordrecht D. Reidel).

van Albada, T.S. 1982, *M.N.R.A.S.*, **201**, 939.

van Albada, T.S., Kotanyi, C.G., and Schwarzchild, M. 1982, *M.N.R.A.S.*, **198**, 303.

Villumsen, J.V. 1984, *Ap.J.*, **284**, 75.

Luis A. Aguilar: Observatorio Astronómico Nacional, Apartado Postal 877, 22860 Ensenada, B.C., México.

Rev. Mexicana Astron. Astrof., 21, 99-102 (1990)

SPHERICAL GALAXIES

J. Eduardo Telles, Ronaldo E. de Souza, Julio C. Penereiro

Depto. de Astronomia, Instituto Astronômico e Geofísico, USP, Brazil

RESUMEN. Presentamos fotometría fotográfica de 8 objetos y espectroscopía para 3 galaxias, las cuales son buenos candidatos para galaxias esféricas. Los resultados fotométricos se presentan en la forma de isofotas y de perfiles radiales promedio, de los cuales se derivan parámetros estructurales. Estas observaciones combinadas con parámetros dinámicos obtenidos de observaciones espectroscópicas, son consistentes con el plano fundamental derivado por Djorgovski y Davis (1987).

ABSTRACT. We present photographic surface photometry for 8 objects and spectroscopy for 3 galaxies which are good candidates for spherical galaxies. Photometric results are presented in the form of isophotes and mean radial profiles from which we derived structural parameters. These observations combined with dynamical parameters obtained from spectroscopic observations are consistent with the fundamental plane derived by Djorgovski and Davis (1987).

Key words: GALAXIES-ELLIPTICAL

. INTRODUCTION

The identification of spherical galaxies constitutes a good test for models which :y to represent the formation and structure of elliptical galaxies. Most of these models imit spherical symmetry and distribution of mass following the distribution of light, obeying ı empyrical $r^{1/4}$ law. Therefore, observable parameters for these galaxies may be directly ɔmpared to intrinsic properties obtained by these models.

In the recent years, various programs of surface photometry have provided a large :ound of information (Schombert, 1986; Djorgovski and Davis, 1987; Jedrzejewski, 1987; Dressler t al., 1987; de Carvalho and da Costa, 1988). Considerable progress has also been achieved by inematical observations (Illingworth, 1977; Davies et al., 1987; etc.). These data have raised ıe problem of the manifold of galaxies. Recently Djorgovski and Davies (1987) and Dressler et l. (1987) have extended the Faber-Jackson relation (FJ, Faber and Jackson, 1976) by introducing second parameter named the mean surface brightness <SB>, thus improving previous attempts ɔ explain the residuals of this relation.

In section II we describe the observations and present our photometric and ɔectroscopic results. In section III we discuss the extended FJ relation in terms of a natural ɔnsequence of the Virial Theorem and suggest that the uncertainties must be well understood efore one can confidently use it as an alternative method for determining distances.

I. OBSERVATIONS AND RESULTS

Photographic plates (short and long exposures) in the V bandpass of 8 galaxies, elected by Telles (1989), were obtained using the 1.6 m telescope of Laboratorio Nacional de strofisica (LNA) in Brazil. The plates were digitalized using the PDS microdensitometer of he Observatorio Nacional. Scans of 200 x 200 pixels (0.64 "/pixel) were obtained. Copies of he ESO-B films were also used, when available, to extend the study to the outer regions of he galaxies. Confident data reduction was done with a new package developed for the use in icrocomputers and is fully described by Telles (1989). Comparisons of the mean radial profiles btained in this work with profiles of Jedrzejewski (1987) show that our photometry is accurate ɔ 0.1-0.2 mag. Figure 1 shows radial mean profiles and isophotal maps of the galaxies and able 1 presents the results from the $r^{1/4}$ law fits.

Spectroscopic data were obtained for 4 galaxies using a CCD camera at the Coudé focus. The spectra covered ∿ 230 Å centered at 8600 Å, in the region of Calcium triplet. We hav used a variation of the Fourier Quotient Method to reduce our data (Telles, 1989; and references therein). The results are also presented in Table 1.

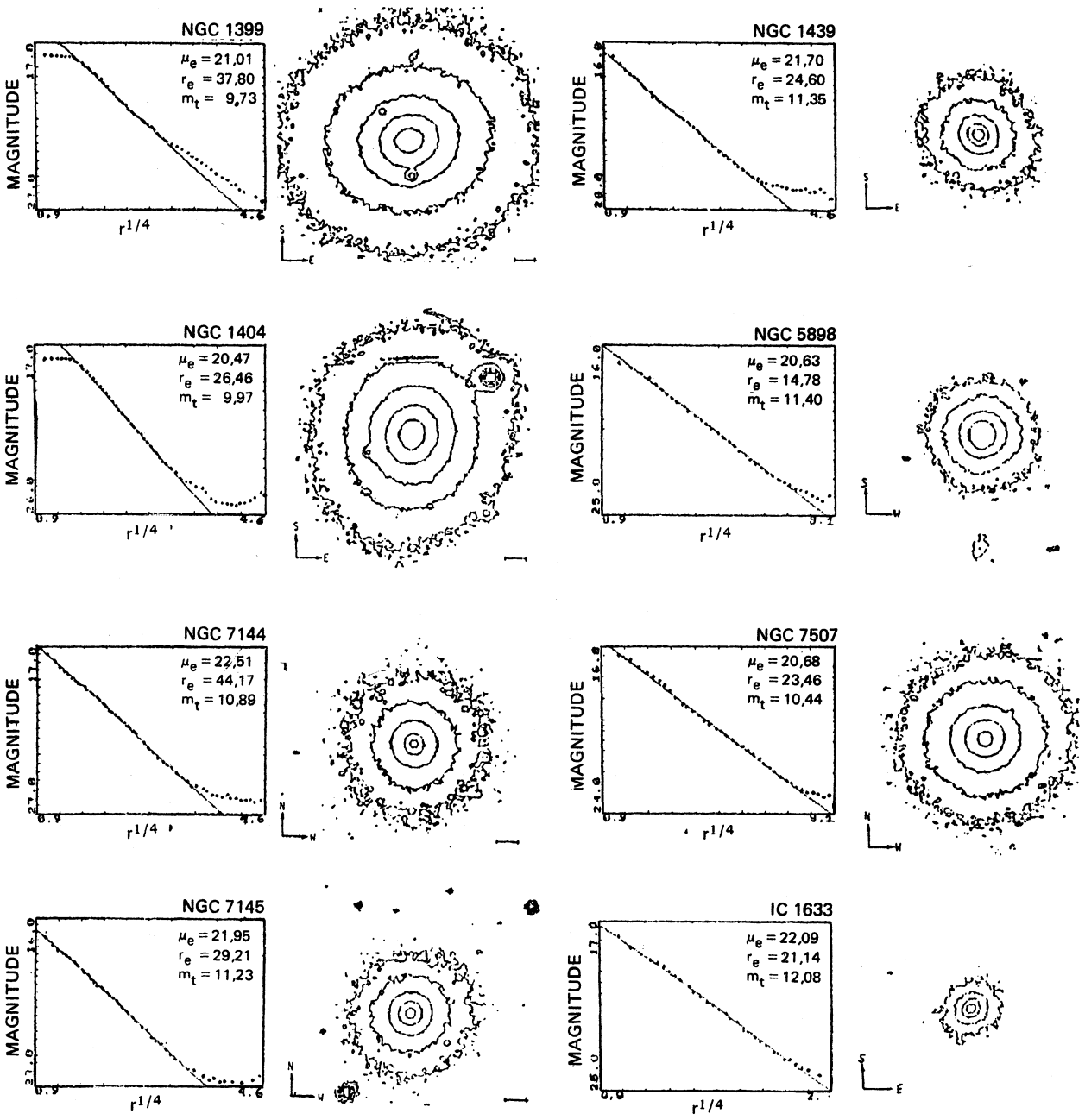

Fig. 1. Mean Radial Profiles vs. $r^{1/4}$ with photometric parameters obtained from best fits (solic lines). Isophotal maps are presented for all 8 objects in intervals of 1 V mag. The innermost isophote represents 18 mag/□. Space orientation and scale bar representing 10 arcseconds are also shown.

ASIC DATA OBTAINED IN THIS WORK

(1) name	(2) type	(3) log(r_e) (")	(4) m_T Vmag	(5) μ_e	(6) $\langle\mu_e\rangle$ (mag/"^{2})	(7) v km/s	(8) logσ km/s	(9) $-M_V$ Vmag	(10) m/L m_o/L_o
N1399	E1cD	1,577	10,48	21,01	19,61	1300	2,462	21,59	3,89
N1404	E1	1,423	10,72	20,47	19,08	1925*	2,352*	22,21	1,38
N1439	E1	1,391	12,10	21,70	20,30	1670*	2,193*	20,52	2,54
N5898	E-S0	1,170	12,15	20,64	19,25	2103*	2,338*	20,97	2,48
N7144	E0	1,645	11,64	22,51	21,11	2020	2,342	21,39	4,90
N7145	E0	1,466	11,98	21,95	20,56	1874*	2,121*	20,89	1,73
N7507	E0	1,370	11,19	20,68	19,29	1650	2,477	21,40	3,93
IC1633	E-S0	1,325	1,283	22,09	20,70	7261	-----	22,98	----

'ABLE 1 - (1) identification; (2) morphological type; (3), (4), (5) effective radius, total agnitude within r_e and effective magnitude at r_e; (6) mean effective magnitude within r_e; 7), (8) radial velocity and velocity dispersion in km/s (* indicates data from Davies et al., 987); (9), (10) absolute magnitude within r_e and mass to luminosity ratios in solar units sing eq. 2.

II. THE FUNDAMENTAL PLANE AND THE M/L RATIO

The numerical coefficients of the relation found by Djorgovski and Davis (1987), $L \alpha \sigma^{3,45} \langle SB\rangle^{-0,86}$, are approximately identical to the values expected by virialized systems. From the 'irial Theorem Poveda (1958) has found, for a spherical, isotropic, pure $r^{1/4}$ law galaxy, in hich mass follows the light:

$$m = 1.55 \frac{1}{G} \sigma^2 R_e \qquad (1)$$

here G is the gravitational constant. After transforming eq. 1 and substituting into solar V nits, we obtain:

$$\log f = 0.2 (M_v + \mu_v) + 2 \log \sigma_{100} + 0.062 \qquad (2)$$

here f is the M/L ratio, M_v and μ_v are the absolute and mean magnitudes within R_e and σ_{100} s the velocity in 100 km/s units.

Therefore, one can expect, for a virialized system, a dependence of the type, $\alpha \sigma^4 \langle SB\rangle^{-1} f^{-2}$, where SB is the mean surface brightness in luminosity units.

We then conclude that the M/L ratio has only a weak dependence on the observable arameters,

$$f \alpha \sigma^{0.28} \langle SB\rangle^{-0.07} \qquad (3)$$

In fact, we have tested this dependence and found, in accordance with other uthours, that it may be spurious in part or in total.

It is interesting to note that if we admit a dependence on the type $f \alpha \sigma^{\alpha} \langle SB\rangle^{\beta}$ hen,

$$L \alpha \sigma^{4-2\alpha} \langle SB\rangle^{-1-2\beta} \qquad (4)$$

here the parameters α and β are near zero and lack a more accurate determination than those vailable from present data base. A more precise definition of these parameters is crucial for better use of the fundamental plane as a distance indicator and a more accurate discussion of he basic properties of the local universe as the velocity field and the large concentration f mass discussed in the literature (Lynden-Bell et al., 1988).

EFERENCES

e Carvalho, R.R., da Costa, L.N. 1988, Ap. J., 160: 173.
avies, R.L., Burstein, D., Dressler, A., Faber, S.M., Lynden-Bell, D., Terlevich, R.J.,

Wegner, G. 1987, Ap. J. Suppl., 64: 581.
Djorgovski, S., Davis, M. 1987, Ap. J., 313: 59.
Dressler, A., Lynden-Bell, D., Burstein, D., Davies, R.L., Faber, S.M., Terlevich, R.J., Wegner, G. 1987, Ap. J. 313: 42.
Faber, S., Jackson, R. 1976, Ap. J., 204: 668.
Illingworth, G. 1977, Ap. J. Letters, 218: 43.
Jedrzejewski, R.I. 1987, M.N.R.A.S., 226: 747.
Lynden-Bell, D., Faber, S.M., Burstein, D., Davies, R.L., Dressler, A., Terlevich, R.J., Wegner, G. 1988, Ap. J., 326: 49.
Poveda, A. 1958, Bol. Obs. Tonantzitla Tacaubaya, 17: 3.
Schombert, J.M. 1986, Ap. J. Suppl., 60: 603.
Telles, J.E. 1989, Dissertação de Mestrado, IAG - Univ. São Paulo.

Julio C. Penereiro, Ronaldo E. de Souza, and J. Eduardo Telles: Departamento de Astronomía, Instituto Astronômico e Geofísico, Universidade de São Paulo, Av. Miguel Stefano, 4200 CEP 04301 São Paulo, SP, Brazil.